References and Notes

(1) (a) S. Ōmura, H. Ohno, T. Saheki, M. Yoshida, and A. Nakagawa, *Biochem. Biophys. Res. Commun.*, **83**, 704 (1978); (b) H. Ohno, T. Saheki, J. Awaya, A. Nakagawa, and S. Ōmura, *J. Antibiot.*, **31**(11), 1116 (1978).

(2) (a) A. Janott, *Annu. Rev. Med.*, **23**, 117 (1972); (b) M. C. Geokas, *Arch. Pathol.*, **86**, 117 (1968).

(3) The structural evidence of **3** was obtained by the following spectral data: δ 176.1 (ester carbonyl carbon), 72.3 (hydroxy carbon), 50.9 (methyne), 22.6–35.6 (seven methylene carbons), 13.9 (two methyl carbons) in the ^{13}C NMR of **4**; typical fragment of *m/e* 241 ($M^+ - OCH_3$), 229 ($M^+ - COCH_3$), 130 (base peak; $CH_3CH_2CH_2CH_2CH{=}C(OH)(OCH_3)$, 87 ($CH_2{=}CHC(=O^+H)(OCH_3)$ in the mass spectrum of **5**.

(4) (a) R. H. Wiley and C. H. Jarboe, *J. Am. Chem. Soc.*, **78**, 624 (1956); (b) D. Herbst, W. B. Mors, O. R. Gottlieb, and C. Djerassi, *ibid.*, **81**, 2427 (1959); (c) J. D. Bu'Lock and H. G. Smith, *J. Chem. Soc.*, **1**, 502 (1960); (d) Y. Koyama, Y. Fukakusa, N. Kyomura, S. Yamaguchi, and T. Arai, *Tetrahedron Lett.*, 355 (1969).

(5) ^1H NMR and ^{13}C NMR spectra of **1** and its derivatives were measured in deuteriochloroform, and IR spectra were obtained in carbon tetrachloride. The assignment of each alkyl carbon in the ^{13}C NMR spectra of all compounds was mainly carried out on the basis of the data listed in J. B. Stothers, "Carbon-13 NMR Spectroscopy", Academic Press, New York, 1972.

(6) Since the hydroxyl carbon of **3** should correspond to the ketone carbonyl of **1**, the following partial structure must be present in **1**.

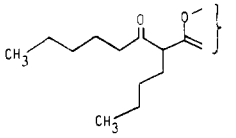

(7) (a) L. C. Dorman, *J. Org. Chem.*, **32**, 4105 (1967). (b) The following mechanism for the production of **6** was speculated:

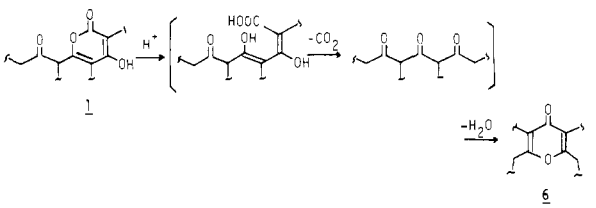

(8) Studies on the protease inhibitors arising from *Streptomyces* have been summarized in the following reviews. (a) T. Aoyagi and H. Umezawa, "Protease and Biological Control", Cold Spring Harbor Laboratories, Cold Spring Harbor, N.Y., 1975, pp 429–454; (b) H. Umezawa, *Methods Enzymol.*, 458, 678–695 (1976); (c) H. Umezawa and T. Aoyagi, "Proteinases of Mammalian Cells and Tissues", A. J. Barrett, Ed., ASP Biological and Medical Press, Amsterdam, 1977, pp 637–662.

S. Ōmura,* A. Nakagawa, H. Ohno

School of Pharmaceutical Sciences
Kitasato University and The Kitasato Institute
Minato-ku, Tokyo 108, Japan

Received February 12, 1979

Upper Excited Triplet State Mechanism in the Trans → Cis Photoisomerization of 4-Bromostilbene

Sir:

The direct trans → cis photoisomerization of stilbene occurs by twisting from 0 to 90° in the lowest excited singlet state, $^1t^*$ → $^1p^*$, followed by internal conversion, $^1p^*$ → ^1p, and twisting from 90 to ~180°, eq 6, in the ground state[1] (for definitions see the explanation of Scheme I). This singlet mechanism for the photoisomerization of stilbene in solution at room temperature is widely accepted.[1-7] However, the discovery of a triplet state of stilbene in rigid matrices[8-10] raises the question as to whether or not a triplet mechanism, as favored by Fischer et al.,[11-13] may contribute to the trans → cis photoisomerization at low temperatures. For 4-bromostilbene, involvement of the lowest triplet state mechanism was postulated by Fischer[11-13] and by Saltiel.[3,5,14] In contrast to unsubstituted stilbene, the quantum yield of fluorescence, ϕ_f, is smaller than 0.2 for *trans*-4-bromostilbene even in rigid glasses at −196 °C.[5,11,15,16]

Using laser flash photolysis,[17-19] we now measured the triplet-triplet absorption spectrum, the triplet lifetime, τ, and the quantum yield of the triplet state, $\phi_{triplet}$, of 4-bromostilbene as a function of temperature in different solvents. The triplet-triplet absorption spectrum is similar to the known spectra of stilbene[8,9] and 4,4′-dichlorostilbene[9] and could be observed below a certain maximum temperature, t_m, without any significant change in shape and λ_{max} down to −196 °C (−80 °C in glycerol and glycerol triacetate (GT), Table I). From this it is concluded that the observed triplet state has the planar trans configuration ($^3t^*$) and that $\phi_{triplet}$ is identified with the yield of formation of $^3t^*$, $\phi_{^3t^*}$.

Scheme I. Upper Excited Triplet Path for Trans → Cis Photoisomerization

$$^1t + h\nu \rightarrow {}^1t^* \quad (1)$$

$$^1t^* \rightarrow {}^3t_h^* \quad (2)$$

$$^3t_h^* \rightarrow {}^3b_h^* \quad (3)$$

$$^3b_h^* \rightarrow {}^3b^* \rightarrow {}^3p^* \quad (4)$$

$$^3p^* \rightarrow {}^1p \quad (5)$$

$$^1p \rightarrow \alpha\,{}^1t + (1-\alpha)\,{}^1c \quad (6)$$

In Figure 1, $\phi_{triplet}$ and τ^{-1} are plotted vs. T^{-1} in comparison with ϕ_f and the quantum yield for the direct trans → cis photoisomerization, $\phi_{t\rightarrow c}$, in a 1:1 mixture of methylcyclohexane and isohexane, MCH-1H. $\phi_{t\rightarrow c}$ does not change from room temperature down to −155 °C, but falls off drastically by further lowering the temperature, and at −185 °C it is too small to be measured. At −155 °C the $^3t^*$ state of 4-bromostilbene appears. The yield of $^3t^*$ increases with decreasing temperature and reaches a constant value at $t_0 = -173$ °C. A comparison of t_m and t_0 values in glycerol and GT with those in the other solvents indicates that viscosity rather than temperature determines the formation of $^3t^*$ (Table I). The lifetime of $^3t^*$ increases in MCH-1H with decreasing temperature from 330 ns at −159 °C reaching a constant value of 0.45 ms below $t_0 = -173$ °C (Figure 1). This is explained by the assumption that the increase in viscosity hinders the $^3t^*$ state from twisting. Therefore, it is suggested that the sharp decrease of $\phi_{t\rightarrow c}$ below −155 °C results from viscosity dependent barriers in both, the upper excited and the lowest triplet states. As shown in Table I, almost the same lifetime of $^3t^*$ is found below t_0 in all solvents examined. Below t_0 no twisting occurs, since $\phi_{t\rightarrow c}$ is zero.

Above −155 °C, trans → cis photoisomerization cannot proceed in the lowest triplet state via $^3t^* \rightarrow {}^3p^*$ since no $^3t^*$ is formed. This follows from the decrease of $\phi_{^3t^*}$ with increasing

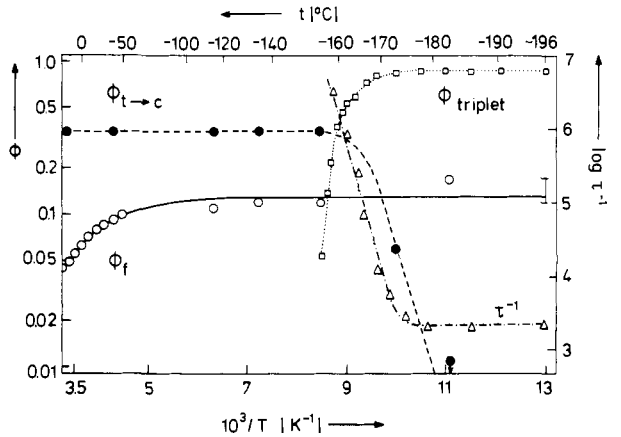

Figure 1. Semilogarithmic plot of $\phi_{t\rightarrow c}$, ϕ_f, $\phi_{triplet}$, and τ^{-1} (in s^{-1}) vs. T^{-1} for *trans*-4-bromostilbene in MCH-1H. ϕ_f values above −50 °C in *n*-pentane are from ref 5 and 21; ϕ_f below −50 °C and $\phi_{t\rightarrow c}$ in MCH-1H are from ref 11-13. At −183 °C, $\phi_{t\rightarrow c} = 0.003$; at 30 °C, a somewhat greater value of $\phi_{t\rightarrow c} = 0.48$ has been found in *n*-pentane.[5] $\phi_{triplet}$ is obtained from optical densities, and a value of $1 - \phi_f = 0.87$ is assumed at −196 °C.

0002-7863/79/1501-4388$01.00/0

Table I. Maxima of Triplet-Triplet Absorption Spectrum, λ_{max}, and Triplet Decay Rate Constants of *trans*-4-Bromostilbene[a]

solvent[b]	λ_{max}, nm[c]	t_m, °C	$10^{-7}k_m$, s^{-1} [d]	t_0, °C	$10^{-3}k_0$, s^{-1} [e]
MCH-1H	*392*, 372, 352	−159	0.3[f]	−173	2.2 (1.7)[g]
MTHF	*392*, 373, 352	−138	5	−169	2.1
EPA	*393*, 372, 355	−143	5	−176	2.0
ethanol	*391*, 372, 352	−130	1[f]	−158	2.1
GT	*390*, 370, 352	−30	3[f]	−66	2.3
glycerol	*395*, 375, 354	+13	3[f]	−64	2.2 (2.6)[h]

[a] *trans*-4-Bromostilbene was the same as in ref 20 and purity was found to be 99.9% by GC. [b] Deoxygenated solutions, ~5 × 10^{-4} M: MCH-1H, methylcyclohexane-isohexane, 1:1; MTHF, 2-methyltetrahydrofuran; EPA, diethyl ether-isopentane-ethanol, 5:5:2; GT, glycerol triacetate. [c] Wavelength of maximum absorption in italics, λ_{exc} 265 nm. [d] First-order decay rate constant at the highest temperature, t_m, amenable to detection. [e] First-order decay rate constant below t_0, specifying the temperature where the straight lines of the temperature-dependent and independent parts of log τ^{-1} vs. T^{-1} cross. [f] Detection at higher temperatures limited by too low a quantum yield of triplet formation. [g] In 3-methylpentane at −196 °C from ref 5. [h] At −78 °C from ref 5.

temperature (Figure 1). At −155 °C, $\phi_{^3t^*}$ is too small to be observed. The lifetime of $^3t^*$ decreases above −173 °C, but does not affect the measurement of $\phi_{^3t^*}$. Between −100 and −150 °C, however, photoisomerization cannot occur exclusively by twisting in the excited singlet state. This follows from the temperature dependence of ϕ_f: Decreasing the temperature leads to an increase of ϕ_f from ≤0.06 at 25 °C to 0.12 at −100 °C.[5,11] This increase is due to a decrease of the activated $^1t^* \rightarrow {}^1p^*$ twisting process,[2,5] perhaps with a contribution of an activated intersystem crossing step. Since further decrease of temperature does not change the value of ϕ_f, no activated process contributes to the decay of $^1t^*$ below −100 °C. Above −155 °C, a radiationless nonactivated decay to the ground state, $^1t^* \rightarrow {}^1t$, should be small since $\phi_{t\rightarrow c}$ is 0.35[11] and $(1 - \alpha)$ is about 0.6.[5] Below −100 °C those excited molecules which do not fluoresce, $1 - \phi_f = 0.87$, should therefore decay by a temperature-independent process to a triplet state. This triplet state cannot be $^3t^*$, since at temperatures above −155 °C this state is not populated. Therefore, it is concluded that between −100 and −155 °C the trans → cis photoisomerization occurs mainly via an upper excited triplet state. As shown in Scheme I, we propose that twisting in the upper excited triplet state, eq 3, is followed by internal conversion, eq 4, intersystem crossing, eq 5, and formation of cis and trans ground states, eq 6.

The symbols t, p, and c refer to the trans, perpendicular, and cis configurations, respectively, superscripts 1 and 3 indicate singlet and triplet states, respectively, subscript h indicates a higher excited state, and α is the fraction of ^1p decaying to ^1t. The symbols $^3b_h^*$ and $^3b^*$ (b, between) represent configurations of an upper excited and the lowest triplet state, respectively, at an angle of twist between 0 and 90°. The angle at which internal conversion $^3b_h^* \rightarrow {}^3b^*$ occurs is considered to be large enough to inhibit population of $^3t^*$. However, the exact angle is not known and may be smaller than 90°. Theoretical calculations by Olbrich[22] for unsubstituted stilbene suggest that the internal conversion occurs at an angle of 20–40° followed by the twisting process $^3b^* \rightarrow {}^3p^*$. This follows from the result that none of the higher excited triplet states below the lowest excited singlet state has a minimum in the potential energy curve at 90°. However, one of these higher triplet states is flat and has a very shallow energy minimum at an angle of 20–40°.

At temperatures above −100 °C, it is suggested that the upper excited triplet mechanism competes with the $^1t^* \rightarrow {}^1p^*$ twisting process. Even at room temperature there should be a contribution of the above upper excited triplet state mechanism, since Saltiel et al. recently reported evidence for substantial quantum yields of intersystem crossing in 4-bromo-, 3-bromo-, and 3,3′-dibromostilbene applying the effect of azulene on cis-trans photoisomerization.[3,5,14] Earlier, Lippert had postulated a $^3t_h^* \rightarrow {}^3c^*$ twisting process in the trans → cis photoisomerization of stilbene.[23,24] However, the arguments advanced are not adequate to permit this conclusion unequivocally, since the presence of a lower lying $^3p^*$ state was not considered.[5] The question arises which upper excited triplet state may be suitable for the twisting process in eq 3 that is expected to be faster than internal conversion, $^3t_h^* \rightarrow {}^3t^*$. It is unlikely that the upper excited triplet state is a vibrationally excited lowest triplet state, since reactions in such states are not probable in the condensed phase. Published calculations of the excited states of stilbene have not included the potential energy curves of all the triplet states that are expected to be below the first excited singlet state.[25-27]

Evidence for the upper excited triplet mechanism is found not only for 4-bromostilbene but also for 4-chloro- and 4-fluorostilbene and unsubstituted stilbene.[28] Owing to increasing ϕ_f values at low temperatures, the contribution of the upper excited triplet mechanism is denreasinoly hronounced in these compounds. The enhancement of ϕ_f at low temperatures in the sequence of Br, Cl, F, and H as substituent is expteined by a decrease of the quantum yield of intersystem crossing due to heavy atom substitution.[5,29] The heavy atom effect rules out a possible alternative for trans → cis photoisomerization by twisting in an excited singlet Franck-Condon state. This pathway would also bypass the lowest triplet and lowest excited singlet states, but a nonactivated process and no influence of a heavy atom effect would be expected.

Acknowledgments. We thank Mr. L. J. Currell for technical assistance and Mrs. R. Straatmann for preparation of 4-bromostilbene.

References and Notes

(1) Saltiel, J.; D'Agostino, J. T.; Megarity, E. D.; Metts, L.; Neuberger, K. R.; Wrighton, M.; Zafiriou, T. C. *Org. Photochem.* **1973**, *3*, 1–113.
(2) Saltiel, J.; D'Agostino, J. T. *J. Am. Chem. Soc.* **1972**, *94*, 6445–6456.
(3) Saltiel, J.; Chang, D. W.-L.; Megarity, E. D.; Rousseau, A. D.; Shannon, P. T.; Thomas, B.; Uriarte, A. K. *Pure Appl. Chem.* **1975**, *41*, 559–579.
(4) Charlton, J. L.; Saltiel, J. *J. Phys. Chem.* **1977**, *81*, 1940–1944.
(5) Saltiel, J.; Marinari, A.; Chang, D. W.-L.; Mitchener, J. C.; Megarity, E. D., submitted for publication in *J. Am. Chem. Soc.* We are obliged to Professor Saltiel for a preprint of this paper.
(6) Pisanias, M. N.; Schulte-Frohlinde, D. *Ber. Bunsenges. Phys. Chem.* **1975**, *79*, 662–667.
(7) Cowan, D. O.; Drisko, R. L. "Elements of Organic Photochemistry"; Plenum Press: New York, 1976; 367 pp.
(8) Heinrich, G.; Blume, H.; Schulte-Frohlinde, D. *Tetrahedron Lett.* **1967**, 4693–4694.
(9) Herkstroeter, W. G.; McClure, D. S. *J. Am. Chem. Soc.* **1968**, *90*, 4522–4527.
(10) Saltiel, J.; D'Agostino, J. T.; Herkstroeter, W. G.; Saint-Ruf, G.; Buu-Hoi, N. P. *J. Am. Chem. Soc.* **1973**, *95*, 2543–2549.
(11) Malkin, S.; Fischer, E. *J. Phys. Chem.* **1964**, *68*, 1153–1163.
(12) Gegiou, D.; Muszkat, K. A.; Fischer, E. *J. Am. Chem. Soc.* **1968**, *90*, 12–18.
(13) Gegiou, D.; Muszkat, K. A.; Fischer, E. *J. Am. Chem. Soc.* **1968**, *90*, 3907–3918.
(14) Saltiel, J.; Chang, D. W.-L.; Megarity, E. D. *J. Am. Chem. Soc.* **1974**, *96*, 6521–6522.
(15) Dyck, R. H.; McClure, D. S. *J. Chem. Phys.* **1962**, *36*, 2326–2345.
(16) Sharafy, S.; Muszkat, K. A. *J. Am. Chem. Soc.* **1971**, *93*, 4119–4125.
(17) Görner, H.; Schulte-Frohlinde, D. *Ber. Bunsenges. Phys. Chem.* **1977**, *81*, 713–720.
(18) Görner, H.; Schulte-Frohlinde, D. *Ber. Bunsenges. Phys. Chem.* **1978**, *82*, 1102–1107.
(19) Görner, H.; Schulte-Frohlinde, D. *J. Phys. Chem.* **1978**, *82*, 2653–2659.
(20) Kuhn, H. J.; Straatmann, R.; Schulte-Frohlinde, D. *J. Chem. Soc., Chem. Commun.* **1976**, 824–825.
(21) Marinari, A.; Saltiel, J. *Mol. Photochem.* **1976**, *7*, 225–249.
(22) Olbrich, G., unpublished results. We thank Dr. Olbrich for placing his results at our disposal prior to publication.
(23) Lippert, E. *Z. Phys. Chem. (Frankfurt am Main)* **1964**, *42*, 125–128.
(24) Krüger, K.; Lippert, E. *Z. Phys. Chem. (Frankfurt am Main)* **1969**, *66*, 293–297.
(25) Borrell, P.; Greenwood, H. H. *Proc. R. Soc. London, Ser. A.* **1967**, *298*, 453–466.
(26) Ting, C.-H.; McClure, D. S. *J. Chin. Chem. Soc. (Taipei)* **1971**, *18*, 95–

107.
(27) Momicchioli, F.; Corradini, G. R.; Bruni, M. C.; Baraldi, I. *J. Chem. Soc., Faraday Trans. 2*, **1975**, 215-224.
(28) Görner, H.; Schulte-Frohlinde, D. submitted for publication in *J. Phys. Chem.*
(29) Muszkat, K. A.; Gegiou, D.; Fischer, E. *J. Am. Chem. Soc.* **1967**, *89*, 4814-4815.

H. Görner, D. Schulte-Frohlinde*
Institut für Strahlenchemie im Max-Planck-Institut für Kohlenforschung D-4330 Mülheim a.d. Ruhr, West Germany
Received January 2, 1979

Ferraborane $B_3H_7Fe_2(CO)_6$, a Diiron Analogue of Pentaborane(9)

Sir:

Recently we reported comparisons of the electronic structure[1] and photochemistry[2] of the five-atom, nido ferraborane, $B_4H_8Fe(CO)_3$,[3] with that of the related compounds B_5H_9 and $C_4H_4Fe(CO)_3$. The aim of this work was to define more precisely the various roles of a metal atom in a cage environment. We now report the preparation and characterization of $B_3H_7Fe_2(CO)_6$,[4] a compound that is also formally a five-atom, 14-electron (nido) cage. Structural characterization permits a test of the prediction that the geometrical structure of B_5H_9 should serve as an adequate model for the structure of the B_3Fe_2 cage.[5] In addition this new compound provides an opportunity to examine the iron-iron interaction in a cage environment.[6]

The preparation of $B_3H_7Fe_2(CO)_6$ from B_5H_9, $Fe(CO)_5$, and $LiAlH_4$ was carried out in a manner similar to the preparation of $B_2H_6Fe_2(CO)_6$.[7] The major differences were that the solvent was changed to 1,2-dimethoxyethane and the temperature to 60-70 °C. Under these conditions an ~1% yield of $B_3H_7Fe_2(CO)_6$ is produced as the major ferraborane containing two iron atoms. The new compound is a volatile, orange, crystalline solid at room temperature that melts at 51 °C. It appears air sensitive but thermally stable in that several samples were kept at 45 °C for 2 months with no evidence of decomposition.

The new compound has the molecular formula $Fe_2B_3C_6O_6H_7$ ($^{56}Fe_2{}^{11}B_3{}^{12}C_6{}^{16}O_6{}^{1}H_7{}^{+}$, calcd 319.922 amu, obsd 319.921 amu). The parent ion in the mass spectrum fragments by the sequential loss of six CO molecules and the envelopes of the parent ion and first three fragment ions are consistent with a molecule containing three boron atoms. The $Fe_2{}^{+}$ ion is prominent in the fragmentation pattern. The infrared spectrum of a film exhibits bands at 2105 (w), 2060 (sh), 2035 (m), 1955 (m) cm^{-1}. There was no evidence for bridging carbonyls. The 100-MHz ^1H FT NMR spectrum in CD_2Cl_2 exhibits two broad resonances (170 Hz, fwhm) at δ −2.6 and −16.6. On ^{11}B decoupling the two resonances sharpen considerably (30 Hz, fwhm) and a similarly sharp resonance appears at δ 3.0. The relative areas of the decoupled signals are 2 (δ 3.0) to 3 (δ −2.6) to 2 (δ − 16.6). The 32.1-MHz ^{11}B FT NMR spectrum consists of four resonances that are analyzed as an overlapping doublet (160 Hz, area 2) and quartet (170 Hz, area 1) at 4.2 and 12.1 ppm, respectively.[8] On ^1H decoupling singlets appear at 4.2 and 12.1 ppm with relative areas of 2 and 1. These data show that the molecule contains the $Fe_2(CO)_6$ fragment, two Fe-H-B bridges, a pair of equivalent borons each coupled to one proton, one boron coupled to three magnetically equivalent protons, and two sets of two and one set of three equivalent protons. These data allow several structural possibilities; thus, a single-crystal X-ray diffraction study was carried out.

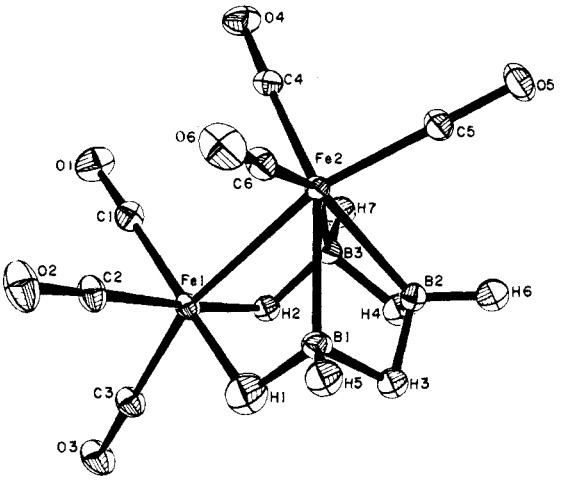

Figure 1. Structure of $B_3H_7Fe_2(CO)_6$.

A crystal 0.8 × 0.3 × 0.4 mm was grown by annealing a polycrystalline sample at 45 °C. The crystal was monoclinic (space group $P2_1/c$, No. 14) with a = 9.006 (2), b = 10.878 (2), c = 12.479 (2) Å; β = 99.54 (1)°. Assuming Z = 4, d_{calcd} = 1.77 g/cm^3. The iron atoms and 10 of the light atoms were located by direct methods using the MULTAN package.[9] The rest of the nonhydrogen atoms were located by Fourier techniques and the model was refined to convergence assuming the atoms to vibrate anisotropically. The hydrogen atoms were located from a difference electron density map and included in the model as isotropic atoms. Two cycles of full-matrix least-squares refinement (based on the 2825 reflections with $F_o > 3\sigma F_o$ and $\sin\theta/\lambda \leq 0.69$) resulted in convergence with a conventional R value of 0.044 and a weighted R value of 0.059.

The structure of $B_3H_7Fe_2(CO)_6$ is shown in Figure 1. The atoms, including hydrogens, are represented as 50% thermal elipsoids. The bond distances in the borane unit are normal:[10] B-B, 1.773 (7) and 1.783 (7); $B-H_{terminal}$, 1.01 (5) to 1.09 (5); $B-H_{bridge}$ 1.19 (5) to 1.33 (4) Å. The Fe-Fe distance is 2.559 (2) which is in the range found for compounds considered to have an iron-iron single bond.[11] The three unbridged Fe(2)-B distances are nearly the same (2.050 (5), 2.062 (4), and 2.070 (5) Å) and are comparable with one unbridged Fe-B distance in $B_5H_8Fe(CO)_3^-$ [12] and $Cu[P(C_6H_5)_3]_2B_5H_8Fe(CO)_3$[13] (2.08, 2.08 Å) but smaller than the other (2.16, 2.15 Å). The two bridged Fe(1)-B distances (2.250 (4) and 2.273 (5) Å) are distinctly longer than the bridged Fe-B distance in the above two monoiron compounds (2.13, 2.12 Å). The $Fe(1)-H_{bridge}$ distances (1.57 (4) and 1.58 (5) Å) are nearly equal to those in the two monoiron compounds (1.52, 1.56 Å), while the boron to Fe-H-B bridging hydrogen distances (1.33 (6) and 1.26 (4) Å) are within the range found for B-H-B bridges. Thus, except for the distortion[14] caused by the size of the iron atoms, the cage structure is basically that of pentaborane(9) in which an apical and a basal BH fragment are replaced by $Fe(CO)_3$ fragments.

The bonding in $B_3H_7Fe_2(CO)_6$ can be viewed in two distinct fashions. The analogy to B_5H_9 stressed above would lead to the valence bond representation sketched in I below in which the

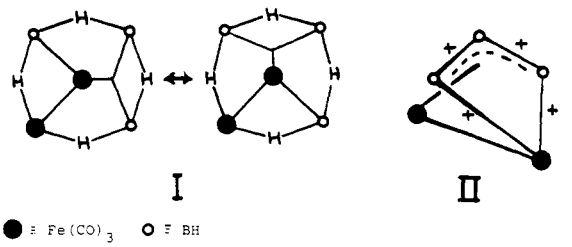

0002-7863/79/1501-4390$01.00/0